A Parametric Study on Nox Emissions From Ammonia Containing Product gas in Rich Quench Lean Combustion

Ahmed Raslan[1]
Department of Mechanical Engineering,
McGill University,
817 Rue Sherbrooke O,
Montréal, Québec, Canada
email: ahmed.raslan@mail.mcgill.ca

Silin Yang
Department of Mechanical Engineering,
McGill University,
817 Rue Sherbrooke O,
Montréal, Québec, Canada
email: silin.yang@mail.mcgill.ca

Antoine Durocher
National Research Council,
1200 Montréal Road,
Ottawa, Ontario, Canada
email: antoine.durocher@mail.mcgill.ca

Felix Güthe
Phoneix Biopower,
Drottning Kristinas väg 14,
Stockholm, Sweden
email: felix.guethe@phoenixbiopower.com

Jeff Bergthorson
Department of Mechanical Engineering,
McGill University,
817 Rue Sherbrooke O,
Montréal, Québec, Canada
email: jeff.bergthorson@mcgill.ca

Due to climate change, there has been an increasing demand for fuels that can accelerate the transition away from fossil fuels to clean energy. Humidified product gas obtained from gasifying biomass is emerging as a promising candidate to replace natural gas, as it is composed of a gaseous mixture of hydrogen, steam, carbon monoxide and methane. However, the gasification process releases ammonia and other nitrogen bearing compounds into the product gas, resulting in substantial increases in nitric oxides, NO_x, in the exhaust. As such, there has been a recent push to understand the underlying chemical kinetics that drive NO_x formation in order to optimize gas turbines to mitigate emissions at the source. In this study, a simplified CRN model for a gas turbine Rich-Quench-Lean (RQL) combustor was developed in Cantera. The following parameters were investigated in this study: equivalence ratio of the primary section, overall equivalence ratio, steam dilution, post flame residence time and recirculation from the post quench region to the primary section. Additionally, a benchmark CRN representing a Lean Burner (LB) as also developed. Results of the CRN model suggest that, when comparing to LB, a RQL type combustor delivers up to a 75% reduction in emissions. Additionally, it was found that, for both the LB and RQL combustors, an overall lean to stoichiometric equivalence ratio is well suited to reduce emissions in highly humidified fuels, while for moderately humidified fuels it is preferable to operate in an overall slightly rich equivalence ratio. The difference observed is mainly due to the fact that, at high humidification and lean conditions, the temperature is favourable for the conversion of ammonia to nitrogen. While, at moderate humidification and rich conditions, NO reacts with ammonia in the reburn process. Finally, it is suggested that the incorporation of recirculation from the secondary section to the primary section of the RQL burner results in a broader low emission region, due to more favourable conditions for ammonia conversion to nitrogen in the primary section.

Keywords: Chemical Reactor Modelling, Ammonia Combustion, Product Gas, Rich Quench Lean

1 Introduction

As the climate crisis threat looms greater by the day, the need for a net-zero fuel to replace natural gas for power generation purposes has never been greater. Product gas is obtained by gasifying biomass into hydrogen, methane and carbon monoxide. However, gasifying biomass results in substantial amounts of ammonia and other Fuel Bound Nitrogen compounds (FBN) being released into the product gas. These compounds can cause a drastic increase in the amount of NO_x produced when combusted [1]. As such, for biomass derived product gas to be considered as a suitable alternative to natural gas, NO_x emissions must be properly characterized and addressed via modifications to the combustors and gas turbine cycles. One such cycle being developed is the Biomass-fired Top Cycle (BTC) developed by Phoenix Biopower [2]. The BTC utilizes a combination of high pressures and humidification using steam in lieu of excess air to control the temperature of the combustor to avoid the formation of NO_x.

NO formation can occur through multiple pathways: these are the thermal Zeldovich pathway (observed in high temperature flames), the prompt pathway (observed for rich hydrocarbon flames), the NNH pathway (prominent for rich conditions at higher temperatures [3]), the N_2O pathway (observed for lean, high pressure conditions and moderate temperatures) and the FBN pathway [4]. As such, the kinetics of ammonia-methane combustion are quite complex, involving interactions between multiple pathways, as outlined by Glarborg et al. [4].

Ammonia can oxidize into multiple intermediates, with the eventual formation of either NO or N_2. NO formation from ammonia is primarily through two intermediates, HNO and NH, while N_2 formation is through either NH_2, NNH, N or N_2O. NO can then be reduced to N_2 through multiple process, including thermal $DeNO_x$, which involves reactions of NO with ammonia products (NH_2 or NH) or, when at low temperatures, the reverse of the thermal NO pathway, $N + NO \rightleftharpoons N_2 + O$. This reversal is possible because the aforementioned reaction has a high activation energy for the backward direction, and as such the forward reaction is favoured at lower temperatures [4].

Thermal $DeNO_x$ is predominantly observed when the mixture is burned at rich conditions. This is because, at rich conditions, ammonia products are more readily available to participate in the $DeNO_x$ process, as shown by Yang et al. [5]. At these conditions, NO is produced at concentrations exceeding that of equilibrium, before relaxing to the equilibrium concentration. Consequently, the residence time of the reactor must be increased to allow for the reduction of excess NO. This behaviour does not occur in lean ammonia flames. This was verified experimentally by Wang et al. [6], using a turbulent burner with an adjustable reactor length, where tripling the length of the reactor did not result in a measurable change in exhaust emissions at lean conditions.

[1]Corresponding Author.
Version 1.18, September 4, 2024

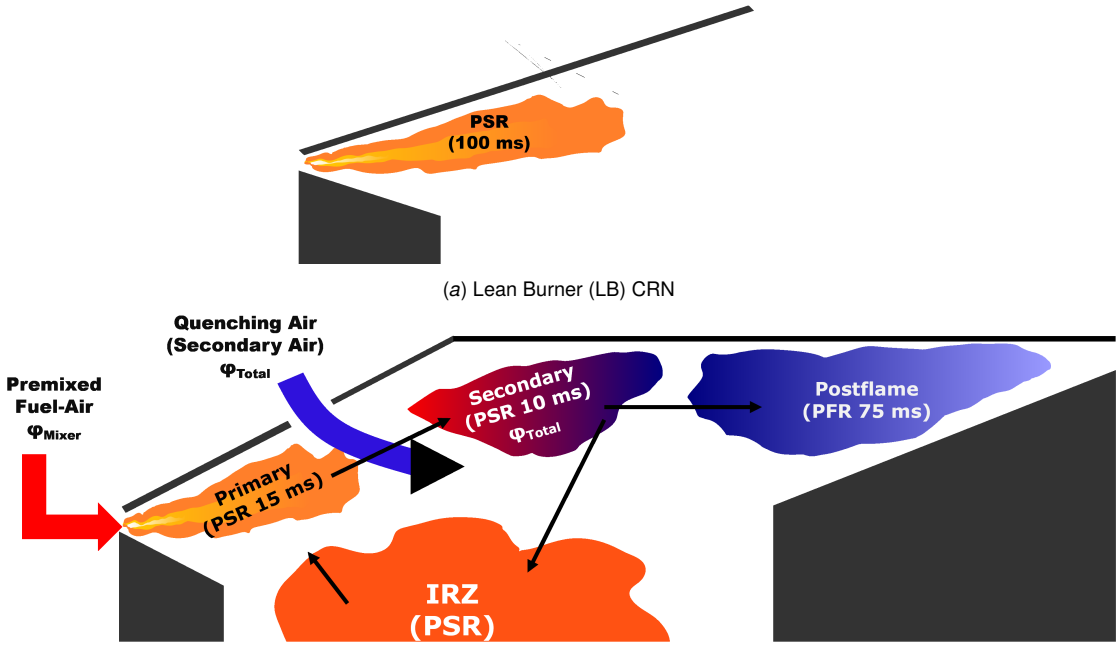

(*a*) Lean Burner (LB) CRN

(*b*) CRN schematic for the Rich Quench Lean combustor

Fig. 1 Configurations of CRNs used in the study

In conventional natural gas and aeroderivative combustors, NO mitigation strategies involve burning a lean premixed fuel and air mixture at a short residence time to avoid the formation of NO through the thermal pathway. Rich Quench Lean burners are also commonly employed to reduce NO_x emissions and soot in gas turbines [7]. These burners work by bypassing the stoichiometric region by initially burning at fuel rich conditions before injecting a secondary supply of air, quenching the flame and shifting the combustion over to the lean burning regime [8]. This reduces the temperature of the combustor, which is integral in avoiding the formation of NO_x. It has been shown experimentally by Kurata et al. [9] that RQL burners are well suited for ammonia combustion, producing as little as 42 ppm of NO. Exhaust gas recirculation, EGR, is another technique commonly utilized in gas turbines in order to combat emissions. It relies on recirculating hot exhaust gas back with the cooler intake gases, this dilutes the concentration of nitrogen and oxygen in the inlet, ultimately reducing the amount of NO produced [10,11]. The mechanism of EGR in gas turbines usually involves internal recirculation between different combustor stages [12]. In this case, recirculation could be driven by swirling the inlet gases, which can also serve to stabilize the flame [13] or reduce emissions [6]. It was shown experimentally by Lipardi et al. [14] that recirculating exhaust gas in methane-air flames reduces NO emissions by slowing down the thermal NO pathway in the postflame. For ammonia-hydrogen flames, it was shown numerically by Masoumi et al. [11] that EGR can reduce NO emissions substantially by lowering the temperature of the reaction, reducing the rate of NO production in the flame.

In this study, the effectiveness of the aforementioned techniques in reducing emissions from ammonia doped product gas combustion will be numerically examined. Additionally, the effect of changing the equivalence ratio, the amount of steam dilution and the recirculation will be studied, with the ultimate goal of finding a range of operational parameters that can mitigate the formation of NO_x at the source.

2 Methodology

Two Chemical Reactor Network models, CRN, were developed in Cantera [15], one for a Rich Quench Lean burner, and the other for a Lean Burner, LB. This study will focus more on having a wide parameter space with the goal of observing trends. The Okafor mechanism [16], which has been shown to provide an adequate representation of FBN chemistry [17], was selected for the simulations. The mechanism is fairly lightweight, containing 59 species and 356 reactions, lowering the computational costs. The mechanism's performance was validated against more complex ammonia-methane mechanisms in the appendix, where it has been shown, at low dilution conditions, that the trends predicted by Okafor are consistent pattern-wise with other mechanisms. However, there exists large discrepancies between mechanisms especially for NO and NH_3 at low temperatures, in terms of emission patterns as well as values. This implies the need for improved models for low temperature ammonia combustion. The LB network scheme is shown in Figure 1(*a*). This CRN consists of a single Perfectly Stirred Reactor, PSR, with a residence time of 100 ms. The RQL CRN consists of a primary section being fed a mix of ammonia and methane, at an equivalence ratio ϕ_{Mixer}, a quenched section with a secondary air injection, followed by a secondary section, at an equivalence ratio ϕ_{Total}, with a postflame of adjustable residence time afterwards. Recirculation is incorporated from the secondary section to the primary section through an Internal Recirculation Zone (IRZ) of negligible residence time. The IRZ was implemented as a reactor in order to ensure the stability of the simulation. This approach is intended to be a geometry agnostic analogy to turbulent phenomena encountered in gas turbine burners, such as flue gas entrainment cause by swirl. All the aforementioned reactors in the RQL CRN are modelled as PSRs with the exception of the postflame which is modelled as a 2000-step Plug Flow Reactor , PFR. The detailed network scheme is shown in Figure 1(*b*). Both reactor networks were evaluated in terms of steam dilution, Ω, and equivalence ratio, ϕ_{Total}.

The residence time of the primary and secondary sections of the network is kept constant by adjusting the volumes of the individual reactors, with the desired residence time being kept at around

25 ms. The primary and secondary sections have a residence of roughly 15 and 10 ms, respectively. To maintain a constant residence time in the PSRs the volume, V, was calculated using the following relationship $V = \frac{\dot{m}\tau}{\rho}$, where $\dot{m}$ is the mass flow and ρ is the density. τ is specified and $\dot{m}$ is calculated a priori. The density is initially solved for using a minimization function, with subsequent points using the previous density to estimate the density at the new setpoint. If the drift of the calculated residence time exceeds 0.5 ms the density is solved for once again using a minimization function. This procedure ensures that the residence time remains roughly constant, while maintaining a reasonable computational time. The total mass flow of gasses into the reactor was kept at a constant 20 kg/s, with the mass flow into the primary section and quench region being adjusted to meet the required equivalence ratios. The temperatures and pressures of the primary and secondary air inlets were kept at conditions similar to ones encountered in a gas turbine system (773 K and 40 atm, respectively). The fuel is a blend of 90% methane with 10% ammonia by molar content, this fuel blend was selected as a simplified substitute for the product gas produced by the gasification process. This allows the model to capture ammonia-hydrocarbon chemistry, without being computationally intensive, allowing for a wide range of parameters to be explored. The steam dilution, Ω, is measured as the molar fraction of steam with respect to the inlet gases into the reactor network, $\Omega = X_{\text{Steam, inlet}}$.

To quantify the pollutants from the reactor and account for any unreacted ammonia, a nitrogenous emission index is employed. This is especially germane in low temperature conditions, where there is negligible amounts of NO produced yet ammonia doesn't fully react. The index aggregates the molar fractions of all non-molecular nitrogen bearing species, including ammonia, and applies a factor that adjusts to the number of nitrogen atoms in said molecule, i.e. the concentration of a species such as N_2O will be multiplied by 2 before being added to the index. The formula for the nitrogenous emission index is described by equation 1. A correction factor is then applied to the index in order to correct for 15% oxygen, as well as drying out the mixture to account for varying steam dilution. Note that, for brevity's sake, the dry nitrogenous emission index will be referred to as dry emissions.

$$\mathrm{I_N} = \sum_{i=1}^{n} n_i X_{\mathrm{N}_i} - 2X_{\mathrm{N}_2} \tag{1}$$

$$\text{Dry } \mathrm{I_N} @\ 15\%\ \mathrm{O_2} = \frac{\mathrm{I}_N}{1 - X_{\mathrm{H_2O}}} \frac{0.21 - 0.15}{0.21 - \frac{X_{\mathrm{O_2,exhaust}}}{1 - X_{\mathrm{H_2O}}}} \tag{2}$$

3 Results & Discussion

3.1 Comparison of LB and RQL performance. Figure 2(*a*) shows the patterns of dry emissions of the Lean Burner CRN, along with white lines representing isotherms. The minimum emission point is marked with a ×. The optimal point occurs at slightly rich conditions at a temperature slightly less than 2000 K and has a value of 112 ppm. At lean conditions, there exists a high dependence of the emissions on temperature, with a low emission zone developing between the 1400 K and 1800 K isotherms. At temperatures higher than 1800 K, NO formation from ammonia is drastically increased, with the formation of NO from atmospheric nitrogen further increasing emissions at temperatures greater than 2100 K. At temperatures lower than 1400 K, ammonia is not completely combusted, persisting at the exhaust of the combustor. At rich conditions, the dependence on temperature shifts, with the optimal temperature range being 1800 K to 2400 K. At rich conditions, the lower temperature limit diverges from 1400 K. The divergence is due to the fact that ammonia is not oxidized due to the more scarce radical pool, namely OH, reducing the rate of ammonia breakdown reactions. OH is particularly important as it is responsible for the most important ammonia breakdown reaction: $NH_3 + OH \rightleftharpoons H_2O + NH_2$. The concentration of OH in the exhaust of LB is plotted in Figure 3 and one could note how the trends in OH concentration are opposite to that of ammonia, confirming that the scarcity of OH when at rich conditions is responsible for the increase in the amount of unburnt ammonia in the exhaust.

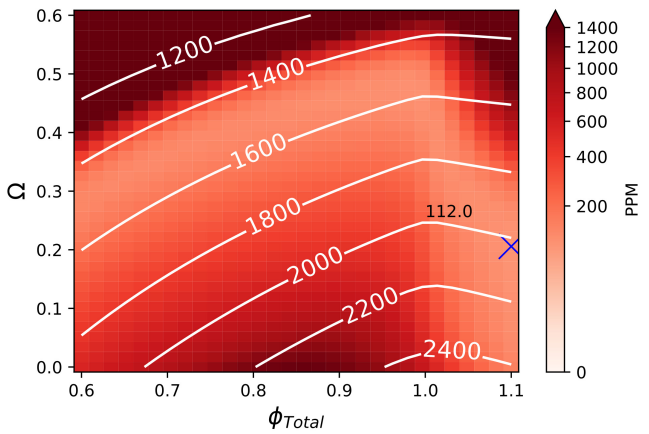

(*a*) LB CRN dry nitrogenous emissions, the blue × indicates the minimum point of nitrogenous emissions in the exhaust

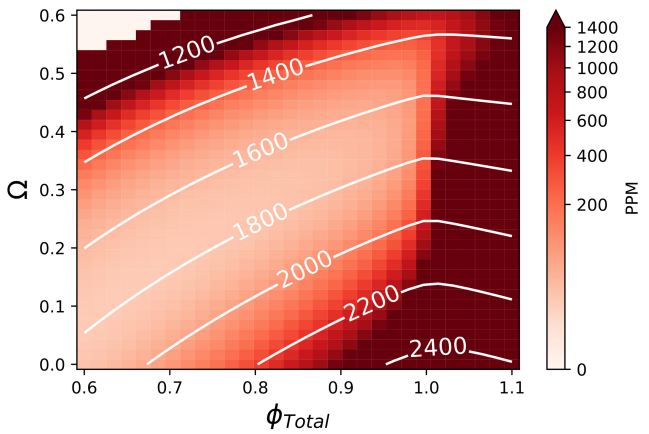

(*b*) LB CRN CO emissions

Fig. 2 LB emissions, isotherms are shown in solid white lines

Figure 4(*a*) shows the patterns of dry emissions of the RQL CRN, with no recirculation and a $\phi_{\text{Mixer}} = 1.3$. The trends observed from the RQL are very similar to that observed from the LB case, with a low emission region forming the shape of an inverted v. At lean conditions, there exists a low emission zone between the 1400 K and 1600 K isotherms. This is because at temperatures greater than 1600 K, NO formation from ammonia is drastically increased, while at temperatures lower than 1400 K ammonia is not completely oxidized, persisting in substantial concentrations at the exhaust of the combustor. At rich conditions, the low emission zone is between 1800 K and 2400 K. Similarly to the LB case, the optimal point occurs at slightly rich conditions at a temperature slightly less than 2000 K. However, the simulated emissions observed are much lower, at only 28 ppm, a reduction of 75%. This indicates that an RQL type combustor is well suited for ammonia doped product gas, as previously indicated in literature [9,18].

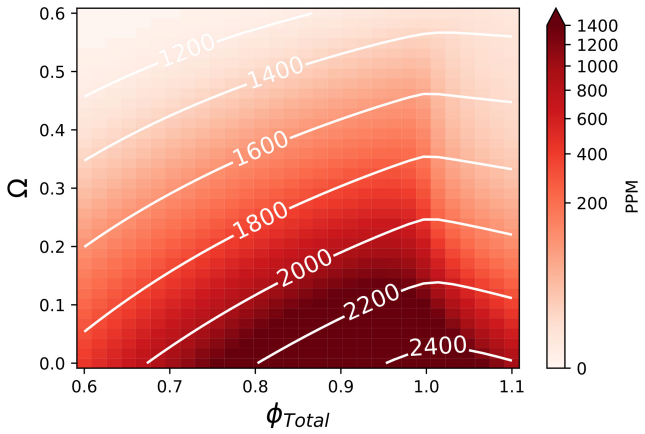

Fig. 3 OH concentration in the LB exhaust, isotherms shown in a solid white lines

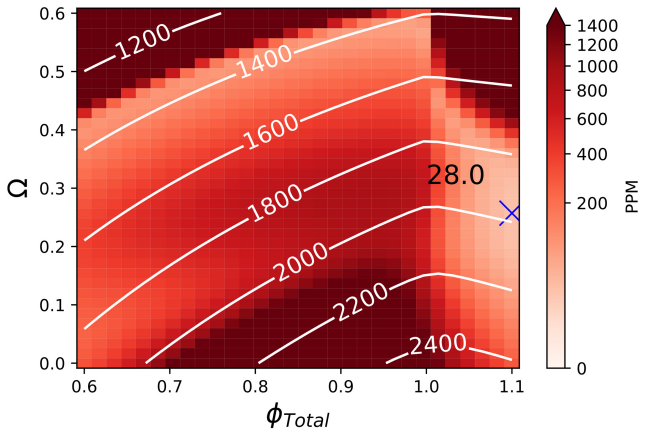

(*a*) RQL CRN dry nitrogenous emissions, isotherms are shown in solid white lines, the blue × indicates the minimum point of nitrogenous emissions in the exhaust

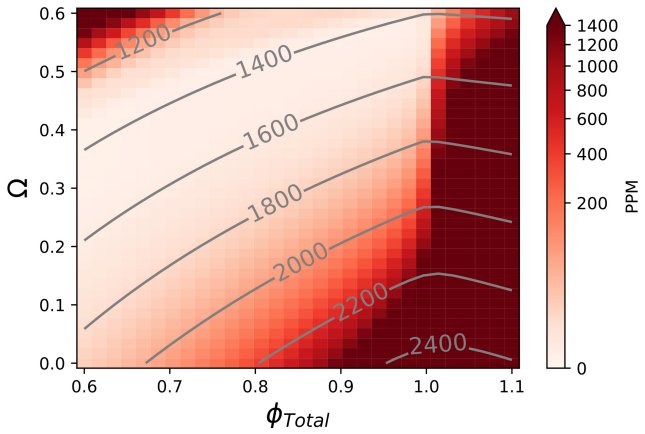

(*b*) RQL CRN CO emissions, isotherms are shown in grey lines

Fig. 4 RQL emissions

The tradeoff between CO and nitrogenous emissions is a well known problem in the gas turbine community [18], as long residence times favour the reduction of CO while, short residence times are favoured to reduce NO from the thermal pathway. As such, CO emission in the RQL and LB CRNs were examined. Figures 2(*b*) and 4(*b*) show the patterns of carbon monoxide emissions in the LB CRN and RQL CRN, respectively. The solid lines represent the isotherms. The patterns of CO emissions in the LB and RQL are quite similar, with the CO concentrations being the highest at rich ϕ_{Total} and slightly lean ϕ_{Total} at temperatures above 2200 K. This implies that the low dilution rich combustion mode, while resulting in lower nitrogenous emissions than the highly diluted lean mode, produces orders of magnitude more CO than the high dilution lean mode. This would necessitate the addition of catalytic reducers or a tertiary air injection to abate the high amount of CO being produced from said combustion mode.

The RQL burner outperforms the LB when it comes to CO emissions. This is quite evident from Figure 4(*b*) CO is almost absent from the RQL exhaust at lean conditions for temperatures between 1200 K and 2000 K.

Results from the LB and RQL CRNs suggest that there exists two viable modes for low nitrogenous emission combustion, these are, burning rich at low dilution or burning lean at high dilution. These modes are summarized in Table 4

Table 1 Summary of low nitrogenous emission combustion modes

Combustion Mode	Advantages	Disadvantages
Low dilution rich combustion	Low NO Production, high peak cycle temperature and plant efficiency, good flame stability	High CO production, wasted fuel
High dilution lean combustion	Low NO Production, Low CO Production, no wasted fuel	Low peak cycle temperature and plant efficiency, poor flame stability

3.2 Recommended residence times for different combustion modes. Figure 6 shows the ratio of NO concentration in the RQL exhaust to the equilibrium NO concentration, $\frac{X_{\text{NO}}}{X_{\text{NO,equilibrium}}}$, the areas shaded blue indicate a ratio that is less than 1, that is sub-equilibrium NO production, conversely the areas shaded red indicate a super-equilibrium NO production. This is a useful tool to determine how long the residence time of the reactor should be, as super-equilibrium NO production would favour a long residence time whereas sub-equilibrium NO production favours a short residence time. The RQL was evaluated at ϕ_{Mixer} = 1.3 and no recirculation. Figure 6 also shows the 1400 K isotherm, which, as observed from the LB and RQL simulations, is the cutoff for quick ammonia breakdown kinetics. As such, burning at temperatures lower than 1400 K should not be considered due to the large amount of unburnt ammonia in the exhaust. At rich conditions, super-equilibrium NO is produced, necessitating a long residence time to allow for NO reduction to occur in the postflame. This strategy could have the added bonus of reducing CO as well, as longer residence times favour CO reduction. At lean conditions and low dilution, it is preferable to burn at a low residence time to mitigate NO formation in the postflame. On the other hand, at highly diluted lean conditions, it would be preferable to burn at moderately long residence times due to the slower ammonia breakdown kinetics, necessitating a longer residence time. NO, production at said conditions is somewhat abated by the lower temperature of the reactor, slowing down NO formation significantly.

The RQL chemical reactor network (CRN) was then further evaluated by varying the primary equivalence ratio, ϕ_{Mixer}, and overall equivalence ratio, ϕ_{Total}. The effect of recirculation from the secondary section to the primary section was also examined, at two different dilution levels, 25% and 50%. These conditions were selected because they are representative of both clean ammonia combustion modes, the lean low dilution mode and rich high dilution mode. The full range of parameters varied in the study for the low and high dilution cases are tabulated in table 5.

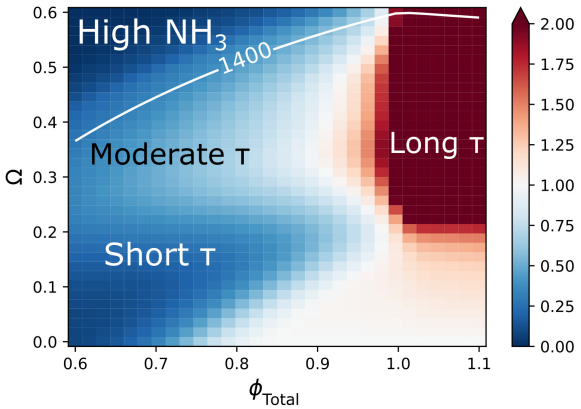

Fig. 6 Ratio of NO concentration in the RQL exhaust to equilibrium NO conentration, 1400 K isotherm shown in a solid white line, highlighting the cutoff for high unburnt ammonia concentration

Table 2 Parameters investigated for the low and high dilution cases

Ω	ϕ_{Mixer}	ϕ_{Total}	Recirculation
0.25	1.1-1.6	0.6-1.1	0 and 0.4
0.5	0.8-1.6	0.6-1.1	0 and 0.4

3.3 Results from low dilution RQL (25%). Figure 5 shows the evolution of emissions across the RQL combustor, at low dilution, broken down by the primary section, secondary section and postflame, with Figures 5(*a*) and 5(*b*) showing the 0% recirculation and 40% recirculation case, respectively. It can be noted that both cases have their optimal dry emission zone of around 28 ppm at slightly rich ϕ_{Total}, which is consistent with the results from Figure 4(*a*). This low emission zone shows no dependence on the primary equivalence ratio ϕ_{Mixer}.

It is observed, from Figs. 5(*a*) and 5(*b*), that the primary section is highly influential on the patterns of emissions in the postflame. This is particularly evident when recirculation is added, resulting in the creation of a low emission zone at a lean ϕ_{Total} in the primary section, which then persists across the reactor. Unlike the low emission zone at rich ϕ_{Total}, this low emission zone is highly sensitive to the ϕ_{Mixer}. This change in emission pattern is due to the fact that recirculation increases the temperature of the primary section, as well as leaning out the composition in the primary section by recirculating additional air from the secondary section. Figure 5b1 plots the effective equivalence ratio, $\phi_{\text{Effective}}$, in the primary section, where a low emission zone is observed between $\phi_{\text{Effective}}$ = 1 and 1.1. This shift in equivalence ratio results in more optimal combustion in the primary section, resulting in a reduction of emissions. However, even after recirculation is added, burning lean at low dilution produces much more emissions than when burning rich.

Both Figures 5a2 and 5a3, as well as 5b2 and 5b3 show that there is significant reduction of emissions in the postflame at slightly rich ϕ_{Total}. Whereas, at lean ϕ_{Total}, there is an increase in emissions in the postflame region. This is consistent with the observations from Figure 6, which indicate that, at lean conditions and low dilution, there is sub-equilibrium production of NO, resulting in production of NO in the postflame. Hence, a long postflame residence time is unnecessary, if not counterproductive, for that low dilution lean conditions. Figure 7(*a*) gives a more detailed snapshot of said reduction in emissions, plotting the temporal evolution of NO and ammonia across the postflame at ϕ_{Total} = 1.1 and ϕ_{Mixer} = 1.2. Said point was selected for analysis as it is generally representative of the pollutant reduction process in the postflame region for the low dilution case. The point selected is marked on Figure 5(*a*) with a black solid circle. The reduction of NO is largely responsible for the decrease, with some conversion of ammonia to nitrogen observed. This process occurs fairly slowly over the length of the postflame, requiring 40 ms in the postflame, 65 ms in the combustor overall, to drop emissions from around 250 ppm to 50 ppm. The profile of NO does not seem to level off even after 100 ms in the combustor, indicating the need for a longer residence time in order to reach equilibrium.

The process of NO reduction to nitrogen in the postflame is quite complex, involving multiple pathways and intermediates. To probe

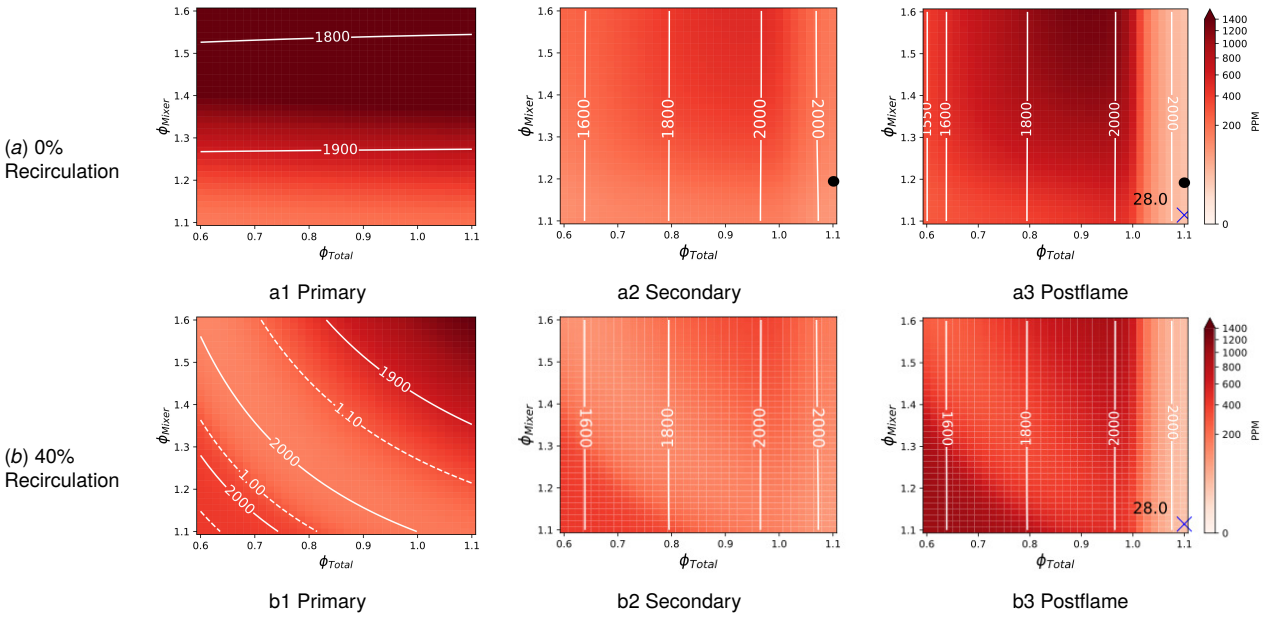

Fig. 5 RQL dry emissions at low dilution (25%), isotherms are shown in solid white lines, actual equivalence ratio, $\phi_{\text{Effective}}$, shown in dashed white lines. The blue × indicates the minimum point of nitrogenous emissions in the exhaust. The black circles on Figures 5a2 and 5a3 mark the point where Reaction Pathway Analysis is conducted.

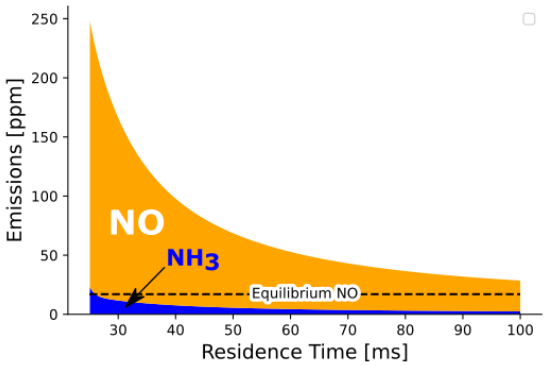

(*a*) NO and NH_3 profiles across the postflame, equilibrium NO concentration plotted with a dashed black line

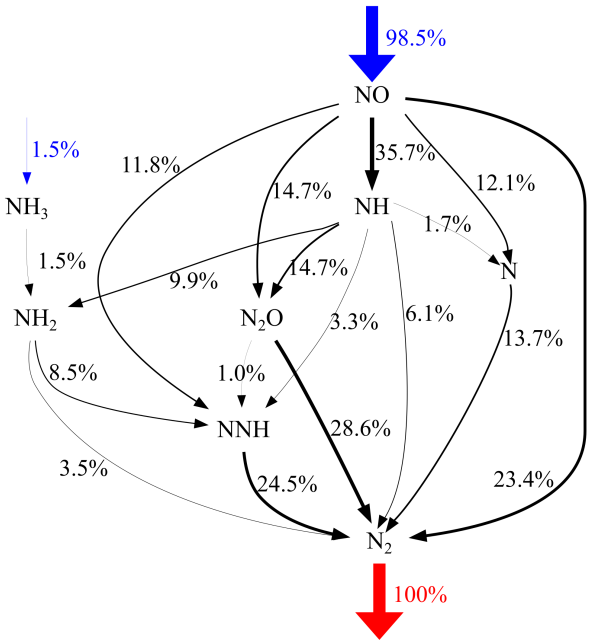

(*b*) Reaction Path Analysis across the postflame

Fig. 7 Post flame Reduction across the postflame, $\phi_{\text{Mixer}} = 1.2$ and $\phi_{\text{Total}} = 1.1$

the process of NO reduction, Reaction Path Analysis, developed by Versailles et al. [19], is used. This tool allows for the tracking of nitrogen flux through different species across a set residence time ($\tau = 25$ ms to $\tau = 100$ ms, which is the length of the postflame). Figure 7(*b*) shows the reaction pathway diagram in the postflame.

NH is an important intermediate in the process of NO reduction, as around a third of NO flux passes by NH. NH can then branch into one of the following intermediates, with the exception of reduction to NH_2 and conversion to N, all the following reactions involve NO. This is because NO is readily available at the inlet of the postflame allowing for the kinetics of these branching reactions to occur quickly:

(1) NH can be reduced to NH_2 via the reverse of the ammonia breakdown process $H + NH_2 \rightleftharpoons H_2 + NH$ or $NH_2 + OH \rightleftharpoons H_2O + NH$. These reactions occur quite readily due to the abundance of water from the flue gas and hydrogen originating from the water gas shift reaction.
(2) NH can be oxidized to N_2O by reacting with NO, $NH + NO \rightleftharpoons H + N_2O$
(3) NH can be converted to N_2 by reacting with NO, $NH + NO \rightleftharpoons OH + N_2$
(4) NH can be converted to NNH by reacting with NO, $NH + NO \rightleftharpoons NNH + O$
(5) NH can be converted to N by reacting with either H or OH, $NH + H \rightleftharpoons N + H_2$, $NH + OH \rightleftharpoons H_2O + N$. Note that both OH and H radicals are quite scarce for rich conditions, which results in this pathway accounting for only 1.7% of the total flux

Almost one quarter of NO is reduced directly via thermal deNO_x reactions ($NH_2 + NO \rightleftharpoons H_2O + N_2$ and $NH + NO \rightleftharpoons N_2 + OH$) or the reverse of the thermal Zeldovich pathway, $N + NO \rightleftharpoons N_2 + O$. N_2O originating from NO can be reduced to N_2 via reaction with OH or via a third body collision, while NNH is converted to N_2 via breakdown to N_2 and H. N is converted to N_2 via the reverse of the thermal Zeldovich pathway $N + NO \rightleftharpoons N_2 + O$. Finally, NH_2 is converted to N_2 via reaction with NO.

The findings from the RPA indicate that NO, NH and OH are particularly important in determining the rate of NO reduction in the postflame. As such, experimentally characterizing their concentration profiles in a flame would be key in order to develop more accurate ammonia-methane combustion models.

3.4 Results from high dilution RQL (50%). To better understand the effect of recirculation, the parameter space for the high dilution case was expanded to include leaner ϕ_{Mixer}. The expanded parameter space is shown in Table 5, note that secondary fuel injections, where $\phi_{\text{Total}} \geq \phi_{\text{Mixer}}$, were not considered. Figure 8 shows the evolution of emissions across the RQL combustor at high dilution broken down by the different component sections, with Figures 8(*a*) and 8(*b*) showing the case with 0% and 40% recirculation, respectively. For both the 0% and 40% recirculation cases, two high emission bands form at slightly rich, $\phi_{\text{Total}} \geq 1.0$, and at very lean, $\phi_{\text{Total}} \leq 0.7$. These bands primarily consist of ammonia. At the rich case, the ammonia is in excess and cannot be oxidized due to the lack of OH radicals across the reactor network. For the lean case, ammonia breakdown kinetics are too slow due to the low temperature of the reactor, resulting in ammonia persisting across the reactor.

The addition of recirculation does not appear to reduce the minimum emission point significantly, with minimum changing from 70 ppm to 66 ppm, with the addition of recirculation. The addition of recirculation shifts the position of the optimum towards a richer ϕ_{Mixer}. Additionally, it can be observed from Figures 8a3 and 8b3 is that normally there is a narrow window of optimal combustion at very lean conditions at $0.85 \leq \phi_{\text{Mixer}} \leq 1$, which broadens to $1 \leq \phi_{\text{Mixer}} \leq 1.4$ with the addition of recirculation. This can be quite useful for gas turbine applications, as one cannot guarantee the mixedness of the fuel and air in the primary stage.

The change in patterns when recirculation is incorporated is due to the primary section being leaned out, as shown in Figure 8b1, which plots the emissions in the primary section as well as the effective equivalence ratio, $\phi_{\text{Effective}}$, in the combustor, shown in dashed lines for the case with 40 % recirculation. The isotherms are also plotted in solid lines. Both Figures 8a1 and 8b1 imply the existence of an upper and lower limit for clean combustion. The lower limit corresponds to the 1400 K isotherm, below which ammonia breakdown kinetics are slow. The upper limit corresponds to a stoichiometric $\phi_{\text{Effective}}$. The addition of recirculation results

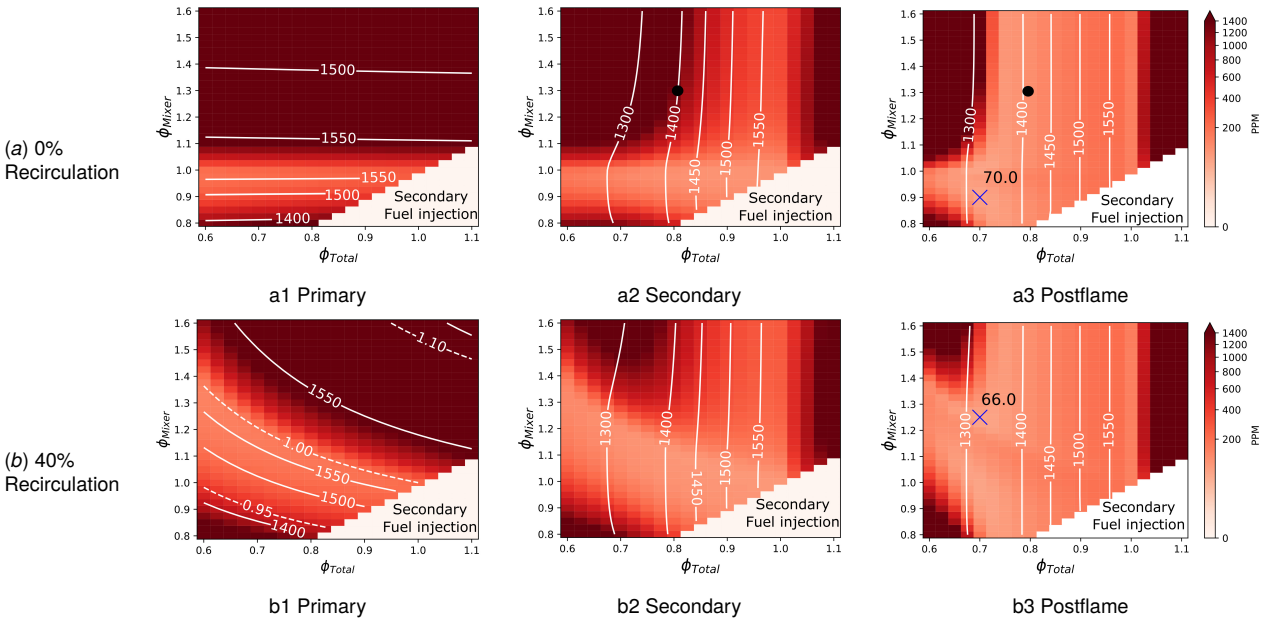

Fig. 8 RQL dry emissions at high dilution (50%), isotherms are shown in solid white lines, actual equivalence ratio, $\phi_{\text{Effective}}$, shown in dashed white lines. The blue × indicates the minimum point of nitrogenous emissions in the exhaust. The black circles on Figures 8a2 and 8a3 mark the point where Reaction Pathway Analysis is conducted.

in broadening the parameter space of optimal combustion in the primary section. This is particularly important for lean ϕ_{Total}, since the temperature in the lean reactor and postflame is below 1300 K, which results in the ammonia breakdown process being frozen.

The high dilution RQL case, whilst providing a better emission profile than that of LB (a reduction of 43% was observed), has an optimal emission point that is double the value of the low dilution case. However, the high dilution case offers a broader combustion range, especially when recirculation is incorporated. Additionally, it also allows for cleaner lean combustion than the low dilution case. This is a desirable characteristic, as burning rich wastes expensive fuel as well as producing a large amount of carbon monoxide. However, the high dilution operating condition has a lower peak temperature, resulting in lower plant efficiency, as well as issues with flame stabilization.

The postflame, similarly to the low dilution case, is responsible for a large reduction in emissions in both the cases with 0% and 40% recirculation. This reduction is most evident at highly rich ϕ_{Mixer} and ϕ_{Total} between 0.7 and 0.9, as can be observed from Figures 8(*a*) and 8(*b*). The reduction profile at $\phi_{\text{Mixer}} = 1.3$ and $\phi_{\text{Total}} = 0.8$ at no recirculation was selected to be shown in more detail in Figure 9(*a*), where the evolution of three most significant nitrogen compounds, NO, NH_3 and N_2O, across the postflame are plotted. The point was selected as it is a good representative of the pollutant reduction process in the postflame of the high dilution case. Said process of reduction is quite quick, when contrasted to the low dilution case, taking only 20 ms to reduce the emissions from >600 ppm to around 70 ppm. It can be noted that the concentration of NO increases very slightly, which is due to the low temperature of the postflame, inhibiting the formation of NO. Instead, the postflame chemistry is dominated by the conversion of ammonia to nitrogen with some reduction of N_2O.

The chemistry of the high dilution postflame is dominated by the conversion of ammonia to nitrogen, accounting for 87.5% of the total flux, as shown in Figure 9(*b*). The main pathways for ammonia oxidation are:

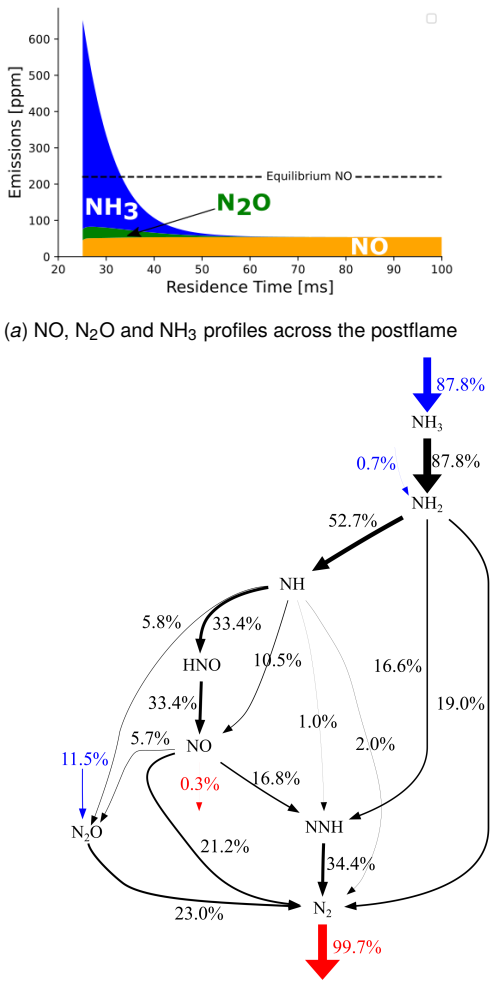

(*a*) NO, N_2O and NH_3 profiles across the postflame

(*b*) Reaction Path Analysis across the postflame

Fig. 9 Postflame evolution of NO, N_2O and NH_3 at high dilution, $\phi_{\text{Mixer}} = 1.3$ and $\phi_{\text{Total}} = 0.8$

(1) Ammonia oxidation to NO, via NH and HNO production, then reduction to N_2 accounting for 43.5% of total nitrogen flux. The reduction of NO to N_2 can then proceed through 3 main pathways, these are:
   (a) Direct reduction to N_2 via $NH + NO \rightleftharpoons N_2 + OH$ accounting for 21.2% of total flux
   (b) Reduction through NNH via $NH_2 + NO \rightleftharpoons NNH + OH$ then oxidation of NNH to N_2 via reaction O_2 $NNH + O_2 \rightleftharpoons HO_2 + N_2$ or a third body reaction with O_2 $NNH + O_2 \rightleftharpoons H + N_2 + O_2$. Said pathway accounts for 16.8% of total flux
   (c) Oxidation to N_2O via $NH + NO \rightleftharpoons H + N_2O$ then reduction to N_2 via a third body collision $N_2O + (M) \rightleftharpoons N_2 + O + (M)$. The pathway accounts for 5.7% of total flux.
(2) Direct ammonia conversion to N_2 via $NH_2 + NO \rightleftharpoons H_2O + N_2$, accounting for 19% of flux
(3) Ammonia conversion to NNH via $NH_2 + NO \rightleftharpoons NNH + OH$ and then NNH oxidation via $NNH + O_2 \rightleftharpoons HO_2 + N_2$ or $NNH + O_2 \rightleftharpoons H + N_2 + O_2$, accounting for 16.6% of flux
(4) Ammonia oxidation to N_2O via $NH + NO \rightleftharpoons H + N_2O$ and then N_2O reduction via $NH + NO \rightleftharpoons H + N_2O$, then reduction to N_2 via a third body collision $N_2O + (M) \rightleftharpoons N_2 + O + (M)$. The pathway accounts for 5.8% of total flux.

Additionally, some N_2O is reduced to N_2, via $NH + NO \rightleftharpoons H + N_2O$ then reduction to N_2 via a third body collision $N_2O + (M) \rightleftharpoons N_2 + O + (M)$, in the postflame accounting for 10.9% of flux. Finally, a very small amount of NO is produced in the postflame through the HNO and NH routes. This due to the low temperature of the postflame resulting in the inhibition of NO forming pathways, and the promotion of nitrogen forming pathways. As with the low dilution case NO, NH and OH all play an important role, with NH contributing to the formation of NO, OH being the main driving force behind the breakdown of ammonia and NO participating in the conversion of various nitrogenous species to N_2.

4 Conclusions

Product gas derived from gasifying biomass is a net-zero alternative for natural gas in gas turbine applications. The gasification process releases substantial amounts of ammonia and other FBN compounds into the product gas, resulting in significant increases in NO_x emissions from the combustion process. In order to counteract this increase in emissions, Phoenix Biopower has developed the BTC, a high pressure steam diluted gas turbine cycle. However, more work needs to be done in order to abate the NO_x emissions from the combustor.

In this study, several burning strategies were investigated in order to reduce emissions from humidified ammonia doped hydrocarbon containing product gas. The fuel mixture consisted of 10% ammonia and 90% methane to simplify the ammonia-hydrocarbon kinetics. The performance of LB and RQL was modelled as CRNs using the Cantera package. Results from the model indicate that the RQL burner outperforms LB, delivering up to a 75% reduction in emissions for the same residence time of 100 ms.

Furthermore, a study was conducted in order to compare the exhaust of the RQL burner to that of equilibrium in order to determine the recommended residence time of the reactor. It was found that, at overall rich conditions, the exhaust concentration of NO is greater than that of equilibrium, necessitating a long postflame to reduce the NO. Whereas, at lean conditions and low dilution, NO is produced quite rapidly, so it is suitable to have a short residence time. Finally, for highly diluted lean conditions, a moderate residence time is appropriate, due to the low temperatures resulting in slow ammonia breakdown kinetics. The low temperatures of the aforementioned case also slow down the NO formation kinetics.

Two main modes of low nitrogenous emission ammonia-methane combustion in gas turbines were identified: low dilution rich combustion and high dilution lean combustion. These two modes were then further investigated in an RQL burner via a parametric sweep of the mixer equivalence ratio, coupled with the addition of recirculation from the secondary section back to the primary section. It was found that recirculation has no effect on the value of the minimum emission point. However, the incorporation of recirculation at low dilution resulted in a low emission zone developing in at lean overall conditions, allowing for cleaner lean combustion than the case with low recirculation. This is because the primary section of the RQL was leaned out, resulting in optimal combustion, reducing NO emissions from ammonia. At high dilution, incorporating recirculation aids in the breakdown of ammonia in the primary section, allowing for heavily leaned out operational conditions. The low dilution case offers a lower optimum nitrogenous emission point of 30 ppm, compared to 65 ppm for the high dilution case. While, the high dilution case offers cleaner lean combustion, free of carbon monoxide emissions.

The kinetics of emissions reduction in the postflame was examined. It was found that, at low dilution and at overall rich conditions, the postflame reduces NO to N_2, with NO, NH and OH playing pivotal roles in the reduction process. This indicates the need for experimental work to verify the underlying kinetics of the formation and consumption of the aforementioned radicals and compounds. At high dilution and lean conditions, the postflame oxidizes ammonia to N_2, reduces N_2O to N_2, with a minuscule amount of NO formation from the ammonia entering the postflame. Similarly to the low dilution case, NO, NH and OH have active roles in both the breakdown of ammonia and the conversion of different nitrogenous species to N_2.

Experimental work should be done to optimize for NO, OH and NH profiles in ammonia-methane flames across different conditions, as said species are quite important for NO formation and reduction. Additionally, further combustion strategies need to be explored, in order to improve on the RQL performance at low steam dilution. This is because, at rich conditions, CO emissions are quite high, with NO emissions being problematic at lean conditions.

Acknowledgment

The author would like to acknowledge the contribution of Phoenix Biopower and financial support from the EUCanWin project and New Frontiers in Research Foundation - Global (NFRF Global) as well as the Fonds de Recherche du Québec (FRQ).

Nomenclature

ϕ_{Mixer} = Equivalence Ratio of the premixer
ϕ_{Total} = Overall Equivalence ratio of the combustor
$\phi_{Effective}$ = Actual Equivalence ratio of the primary section
Ω = Steam dilution
X_i = Molar fraction of specie i
τ = Residence Time
CRN = Chemical Reactor Network
EGR = Exhaust Gas Recirculation
FBN = Fuel Bound Nitrogen
LB = Lean Burner
N_i = Nitrogen bearing specie
n_i = Number of Nitrogen atoms in a specie
I_N = Nitrogenous Emission Index
PFR = Plug Flow Reactor
PSR = Perfectly Stirred Reactor
RQL = Rich Quench Lean

Appendix A: Validation of different Mechanisms

The mechanisms selected to validate Okafor are tabulated in Table 6. The RQL cycle was then simulated using different mechanisms at two values of Ω, 0.25 and 0.5, while varying ϕ_{Total} and

at $\phi_{\text{Total}} = 0.7$ while varying Ω. For all three sweeps the ϕ_{Mixer} and recirculation were kept constant at 1.3 and 40%, respectively. Figure 10 shows the nitrogenous emissions as predicted by Okafor, along with thick black lines that represent where the sweeps were conducted.

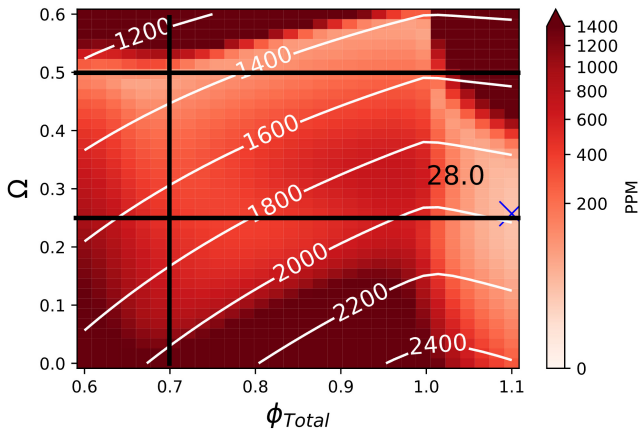

Fig. 10 RQL CRN dry nitrogenous emissions as predicted by Okafor, isotherms are shown in solid white lines, the blue × indicates the minimum point of nitrogenous emissions in the exhaust, the three thick black lines show the parameters where sweeps using different mechanisms were conducted

Table 3 Summary of Mechanisms used for validation

Reference	Name	Species	Reactions
[16]	Okafor	59	356
[20]	Wang	91	444
[21]	Stagni	157	2444
[22]	Reduced NUIG	104	935
[23]	Glarborg	153	1412

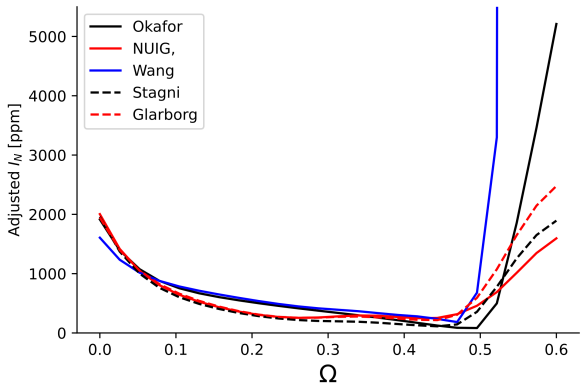

Fig. 11 RQL CRN dry nitrogenous emissions as predicted by different mechanisms at $\phi_{\text{Total}} = 0.7$

Results from $\phi_{\text{Total}} = 0.7$. Figure 11 shows how different mechanisms predict dry nitrogenous emissions in the RQL CRN at increasing steam dilution. The mechanisms are in good agreement, when examining patterns at low dilutions. However, at high dilutions, $\Omega > 0.5$, the mechanisms predict different amounts of unburnt ammonia in the exhaust, with Wang predicting a higher temperature to completely consume ammonia, resulting in a large spike in nitrogenous emissions. This result implies that there is a large uncertainty in the low temperature chemistry of ammonia-methane blends.

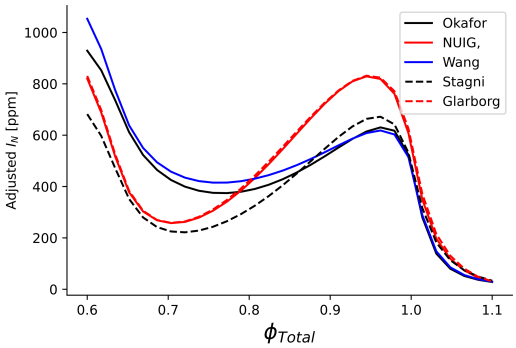

Fig. 12 RQL CRN dry nitrogenous emissions as predicted by different mechanisms at Ω = 0.25

Results from the 25% dilution case. Figure 12 shows how different mechanisms predict dry nitrogenous emissions in the RQL CRN. It can be noted that all the mechanisms display a similar pattern of the two low emission zones. However, the shape and value of the lean emission minima vary by mechanism, with Stagni, Glarborg and NUIG having a local emission minima between 200 and 250 ppm at around $\phi_{\text{Total}=0.7}$. This minima is surrounded by a sharp increase in emissions as you move away from the minimum. Conversely, Okafor and Wang predict higher lean emission minima ranging between 400 and 450 ppm at around $\phi_{\text{Total}=0.75}$, the minima is surrounded by a gentle increase in emissions. A local maximum is predicted by all mechanisms to be around $\phi_{\text{Total}} = 0.95$. However, the value of that local maximum varies by mechanism, with Okafor, Wang and Stagni predicting a local maximum of 600-650 ppm, with NUIG and Glarborg predicting a maximum of 800 ppm. It is interesting to note that at the low dilution case NUIG and Glarborg having very similar profiles. On the other hand, at rich conditions, all mechanisms converge on the same value of dry nitrogenous emissions. This implies that, while there are significant variations between mechanisms, the trends of emissions, at low dilution, remain the same.

Results from the 50% dilution case. Figure 13(*a*) shows how different mechanisms predict dry nitrogenous emissions in the RQL CRN, as well as NO and NH_3, shown in figures 13(*b*) and 13(*c*), respectively, the two most important nitrogen species. At lean conditions, ammonia predictions are consistent for all mechanisms, except for Wang at lean conditions, which predicts a large amount of unburnt ammonia in the exhaust. This is due to Wang having a higher lower temperature limit for the complete oxidation of ammonia. As the mixture moves to rich ϕ_{Total}, the predictions for ammonia start to diverge, indicating there is a large variation in models predicting low temperature ammonia combustion. Conversely, NO predictions show a large discrepancy across different mechanisms at low temperatures, especially at lean conditions, where neither the patterns or magnitude of emissions are consistent. Indicating that NO chemistry from the FBN route is not well understood at low temperatures. However, since this is the high dilution case, NO production is not as high. As such, ammonia ends up dominating the nitrogenous emission patterns, which is more consistently modelled. This results in a nitrogenous emission pattern a that is roughly consistent across different mechanisms as shown in figure 13(*a*).

References

[1] Khateeb, A. A., Guiberti, T. F., Wang, G., Boyette, W. R., Younes, M., Jamal, A., and Roberts, W. L., 2021, "Stability limits and NO emissions of premixed swirl

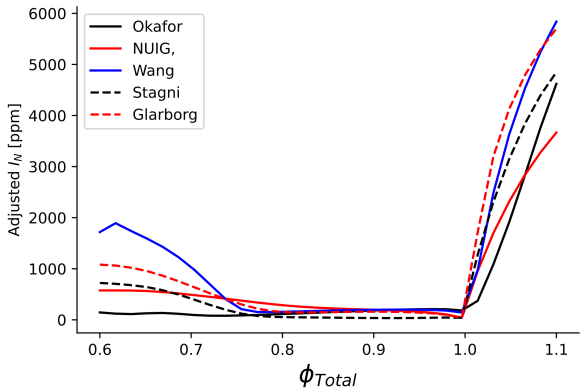

(*a*) RQL CRN dry nitrogenous emissions as predicted by different mechanisms at Ω = 0.5

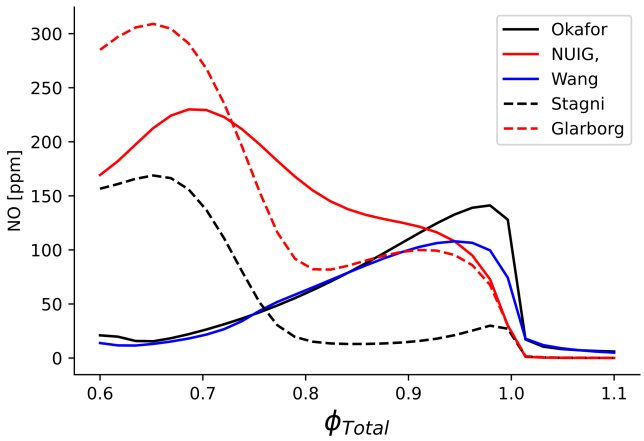

(*b*) RQL CRN NO emissions as predicted by different mechanisms at Ω = 0.5

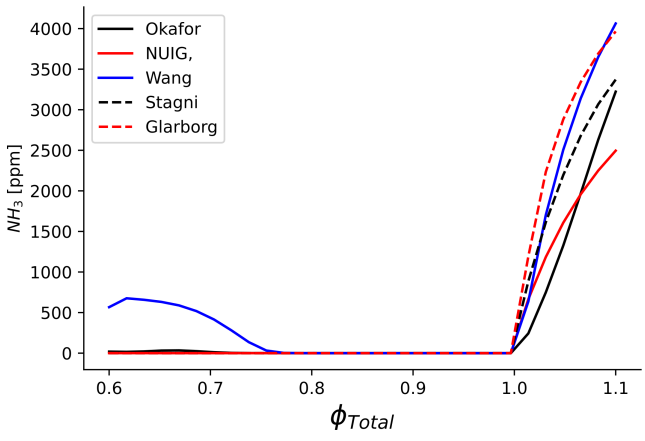

(*c*) RQL CRN NH_3 emissions as predicted by different mechanisms at Ω = 0.5

Fig. 13 RQL CRN emissions as predicted by different mechanisms at Ω = 0.5

ammonia-air flames enriched with hydrogen or methane at elevated pressures," International Journal of Hydrogen Energy, **46**(21), pp. 11969–11981.

[2] Dybe, S., Güthe, F., Bartlett, M., Stathopoulos, P., and Paschereit, C. O., 2021, "Experimental Characterization of the Combustion in Fuel Flexible Humid Power Cycles," **Volume 3A: Combustion, Fuels, and Emissions**, p. V03AT04A012.

[3] Day, M. S., Bell, J. B., Gao, X., and Glarborg, P., 2011, "Numerical simulation of nitrogen oxide formation in lean premixed turbulent H2/O2/N2 flames," Proceedings of the Combustion Institute, **33**(1), pp. 1591–1599.

[4] Glarborg, P., Miller, J. A., Ruscic, B., and Klippenstein, S. J., 2018, "Modeling nitrogen chemistry in combustion," Progress in Energy and Combustion Science, **67**, pp. 31–68.

[5] Yang, S., Raslan, A., Durocher, A., Güthe, F., and Bergthorson, J., 2023, "Numerical Investigation of NH3 Doped Fuels From Biomass Gasification on Fuel-Bound NOx Formation at Gas Turbine Conditions," **Volume 3B: Combustion, Fuels, and Emissions**, p. V03BT04A028.

[6] Wang, G., Guiberti, T. F., Cardona, S., Jimenez, C. A., and Roberts, W. L., 2022, "Effects of residence time on the NOx emissions of premixed ammonia-methane-air swirling flames at elevated pressure," Proceedings of the Combustion Institute.

[7] Samuelsen, S., 2006, "Rich burn, quick-mix, lean burn (RQL) combustor," The Gas Turbine Handbook, pp. 227–233.

[8] Bergthorson, J. M. and Thomson, M. J., 2015, "A review of the combustion and emissions properties of advanced transportation biofuels and their impact on existing and future engines," Renewable and Sustainable Energy Reviews, **42**, pp. 1393–1417.

[9] Kurata, O., Iki, N., Inoue, T., Matsunuma, T., Tsujimura, T., Furutani, H., Kawano, M., Arai, K., Okafor, E. C., Hayakawa, A., and Kobayashi, H., 2019, "Development of a wide range-operable, rich-lean low-NOx combustor for NH3 fuel gas-turbine power generation," Proceedings of the Combustion Institute, **37**(4), pp. 4587–4595.

[10] Hachem, J., Schuhler, T., Orhon, D., Cuif-Sjostrand, M., Zoughaib, A., and Molière, M., 2022, "Exhaust gas recirculation applied to single-shaft gas turbines: An energy and exergy approach," Energy, **238**, p. 121656.

[11] Masoumi, S., Houshfar, E., and Ashjaee, M., 2024, "Experimental and numerical analysis of ammonia/hydrogen combustion under artificial exhaust gas recirculation," Fuel, **357**, p. 130081.

[12] Salzmann, R. and Nussbaumer, T., 2001, "Fuel Staging for NOx Reduction in Biomass Combustion: Experiments and Modeling," Energy & Fuels, **15**(3), pp. 575–582.

[13] Hayakawa, A., Arakawa, Y., Mimoto, R., Somarathne, K. K. A., Kudo, T., and Kobayashi, H., 2017, "Experimental investigation of stabilization and emission characteristics of ammonia/air premixed flames in a swirl combustor," International Journal of Hydrogen Energy, **42**(19), pp. 14010–14018, Special Issue on The 21st World Hydrogen Energy Conference (WHEC 2016), 13-16 June 2016, Zaragoza, Spain.

[14] Lipardi, A. C., Versailles, P., Watson, G. M., Bourque, G., and Bergthorson, J. M., 2017, "Experimental and numerical study on NOx formation in CH4–air mixtures diluted with exhaust gas components," Combustion and Flame, **179**, pp. 325–337.

[15] Goodwin, D. G., Moffat, H. K., Schoegl, I., Speth, R. L., and Weber, B. W., 2022, "Cantera: An Object-oriented Software Toolkit for Chemical Kinetics, Thermodynamics, and Transport Processes," https://www.cantera.org, doi: 10.5281/zenodo.6387882, Version 2.6.0.

[16] Okafor, E. C., Naito, Y., Colson, S., Ichikawa, A., Kudo, T., Hayakawa, A., and Kobayashi, H., 2019, "Measurement and modelling of the laminar burning velocity of methane-ammonia-air flames at high pressures using a reduced reaction mechanism," Combustion and Flame, **204**, pp. 162–175.

[17] Alturaifi, S. A., Mathieu, O., and Petersen, E. L., 2022, "A shock-tube study of NH3 and NH3/H2 oxidation using laser absorption of NH3 and H2O," Proceedings of the Combustion Institute.

[18] Rodolfo C. Rocha, M. C. and Bai, X.-S., 2021, "Combustion and Emission Characteristics of Ammonia under Conditions Relevant to Modern Gas Turbines," Combustion Science and Technology, **193**(14), pp. 2514–2533.

[19] Versailles, P., Watson, G. M., Lipardi, A. C., and Bergthorson, J. M., 2016, "Quantitative CH measurements in atmospheric-pressure, premixed flames of C1–C4 alkanes," Combustion and Flame, **165**, pp. 109–124.

[20] Wang, Z., Han, X., He, Y., Zhu, R., Zhu, Y., Zhou, Z., and Cen, K., 2021, "Experimental and kinetic study on the laminar burning velocities of NH3 mixing with CH3OH and C2H5OH in premixed flames," Combustion and Flame, **229**, p. 111392.

[21] Arunthanayothin, S., Stagni, A., Song, Y., Herbinet, O., Faravelli, T., and Battin-Leclerc, F., 2021, "Ammonia–methane interaction in jet-stirred and flow reactors: An experimental and kinetic modeling study," Proceedings of the Combustion Institute, **38**(1), pp. 345–353.

[22] Curran, H., personal communication.

[23] Li, M., He, X., Hashemi, H., Glarborg, P., Lowe, V. M., Marshall, P., Fernandes, R., and Shu, B., 2022, "An experimental and modeling study on auto-ignition kinetics of ammonia/methanol mixtures at intermediate temperature and high pressure," Combustion and Flame, **242**, p. 112160.

[24] Stagni, A., Cavallotti, C., Arunthanayothin, S., Song, Y., Herbinet, O., Battin-Leclerc, F., and Faravelli, T., 2020, "An experimental, theoretical and kinetic-modeling study of the gas-phase oxidation of ammonia," React. Chem. Eng., **5**, pp. 696–711.

Table 4 Summary of low nitrogenous emission combustion modes

Combustion Mode	Advantages	Disadvantages
Low dilution rich combustion	Low NO Production, high peak cycle temperature and plant efficiency, good flame stability	High CO production, wasted fuel
High dilution lean combustion	Low NO Production, Low CO Production, no wasted fuel	Low peak cycle temperature and plant efficiency, poor flame stability

Table 5 Parameters investigated for the low and high dilution cases

Ω	ϕ_{Mixer}	ϕ_{Total}	Recirculation
0.25	1.1-1.6	0.6-1.1	0 and 0.4
0.5	0.8-1.6	0.6-1.1	0 and 0.4

Table 6 Summary of Mechanisms used for validation

Reference	Name	Species	Reactions
[16]	Okafor	59	356
[20]	Wang	91	444
[21]	Stagni	157	2444
[22]	Reduced NUIG	104	935
[23]	Glarborg	153	1412

List of Figures

List of Tables